Measurement Induced Localization from Spontaneous Decay

M. Holland,[1] S. Marksteiner,[1,2] P. Marte,[1,2] and P. Zoller[1,2]
[1]*Joint Institute for Laboratory Astrophysics and Department of Physics, University of Colorado, Boulder, Colorado 80309-0440*
[2]*Institute for Theoretical Physics, University of Innsbruck, Technikerstrasse 25, A-6020 Innsbruck, Austria*
(Received 13 February 1995)

We present a simulation method which localizes the atomic wave function each time a spontaneous photon is emitted. This allows a small set of basis states to be allocated dynamically to follow the atomic motion. We illustrate the application of this technique in a study of position jumps and quantum diffusion in the laser cooling of atoms. [S0031-9007(96)00228-1]

PACS numbers: 42.50.–p, 03.65.Bz, 32.80.–t

Let us consider the spatially resolved photodetection of fluorescence photons from laser driven atoms. According to quantum measurement theory, each observation of an emitted photon will localize the atomic center of mass wave function in agreement with the spatial resolution of the detection scheme. Continuous observation of these fluorescence photons allows us to give an operational definition of a "quantum trajectory" of a moving atom in terms of the sequence of spatially resolved detection events. This is of direct relevance for the description of the random motion and transport of atoms in optical molasses and atomic traps in the limit where the atomic center of mass motion must be quantized. In this Letter we develop a master equation formulation of this physical picture. Apart from the conceptual interest from the measurement point of view, this formulation leads directly to a novel wave function simulation method where the spatial grid on which the atomic wave function is represented follows the Brownian motion of the atom.

In quantum optics, dissipation of a system may be treated by coupling to an external reservoir. The quantum master equation is derived by tracing over the reservoir states under the Markov approximation. This gives the evolution of the reduced density operator ρ for the system alone [1],

$$\dot{\rho} = -\frac{i}{\hbar}(\hat{H}_{\rm eff}\rho - \rho\hat{H}_{\rm eff}^{\dagger}) + \sum_{\gamma} 2\hat{a}_{\gamma}\rho\hat{a}_{\gamma}^{\dagger}, \qquad (1)$$

where the non-Hermitian effective Hamiltonian $\hat{H}_{\rm eff} = \hat{H} - i\hbar\sum_{\gamma}\hat{a}_{\gamma}^{\dagger}\hat{a}_{\gamma}$ is defined in terms of the Hamiltonian $\hat{H}$ for the isolated system. The operator $\hat{a}_{\gamma}$ when applied to the state generates the effect on the system of a decay into the reservoir mode labeled by γ. In continuous measurement theory, the master equation has the interpretation of describing the time evolution of a system which is continuously observed, but the results of the measurement are not read and no selection is made [2]. Consider, in particular, a system coupled to $\gamma = 1, \ldots, N$ counters which act continuously to register the arrival times of photons. The time evolution of the system conditional to having observed a certain trajectory of counts is described by a system wave function $\psi(t)$ undergoing a sequence of quantum jumps. Between the counts the system state evolves according to $i\hbar\dot{\psi}(t) = \hat{H}_{\rm eff}\psi(t)$ in which the norm $\|\psi(t)\|$ decreases with time from its initial value of unity. The time t' for the next decay can be found by simulating a uniformly distributed random variable R in the interval $[0, 1]$ and solving $\|\psi(t')\|^2 = R$. A second random variable is used to simulate the reservoir mode in which the excitation is observed, assigning a relative weight $\|\hat{a}_{\gamma}\psi(t')\|^2$ to each counter. The operator for the chosen mode is used to generate a quantum jump of the state $\psi(t' + dt) = \hat{a}_{\gamma}\psi(t')$ for infinitesimal dt. This is then renormalized and becomes the initial state for the next interval. The master equation is derived by a stochastic average $\rho(t) = \langle|\varphi(t)\rangle\langle\varphi(t)|\rangle_{\rm st}$ where $\varphi(t) = \psi(t)/\|\psi(t)\|$ is the normalized system wave function. An alternative stochastic formulation is quantum state diffusion [3] which replaces the jumps by a diffusive time evolution and in quantum optics corresponds to homodyne detection.

The formulation of a stochastic evolution in terms of system wave functions has gained considerable interest both as a novel simulation tool for the master equation [4,5], and also from a conceptual point of view since the individual trajectories might be interpreted as what may be observed in a single run of an experiment. In this sense the simulation corresponds to an idealized computer experiment for a quantum optical system. In general, however, there is not a unique way of decomposing the master equation to form quantum trajectories, since the reservoir measurement may be performed in any basis. This statement is equivalent to noting that Eq. (1) is invariant under the substitution $\hat{a}_{\gamma} \to \sum_{\alpha} U_{\gamma\alpha}\hat{a}_{\alpha}$ where U is any unitary transformation [4]. In this Letter, we demonstrate that an appropriate choice of $\hat{a}_{\gamma}$ is crucial for the formulation of an efficient simulation method for estimating the ensemble distribution. Note that the observation of a count in a particular decay channel γ localizes the wave function according to the action of the corresponding $\hat{a}_{\gamma}$. A continuous spontaneous localization also occurs in quantum state diffusion models [3]. The criteria to consider when selecting the measurement basis is that it should be chosen in such a way as to minimize the phase space required to accurately describe the state as the system evolves. As an important example,

we consider in detail the treatment of the spontaneous emission of photons by atoms, although the principle can be extended to relaxation processes in other systems.

Simulation methods for calculating spontaneous emission have predominantly assumed an angle resolved detection of the photon, i.e., the measurement of the wave vector. For a one-dimensional system this gives the decay operators [5]

$$\hat{a}_{u\sigma} = (N_{u\sigma})^{1/2}\hat{A}_\sigma \exp(-iku\hat{x}), \tag{2}$$

where $u \in [-1, 1]$ is the component of the photon's direction vector along the axis of interest. The angular momentum of the photon about this simulation axis is $\sigma = 0, \pm 1$. The wave number of the photon is k, $\hat{A}_\sigma$ is the internal lowering operator proportional to the square root of the transition rate, and $\hat{x}$ is the one-dimensional position operator for the center of mass of the atom. The angular distribution of the radiation pattern is characterized by the functions $N_{u0} = 3(1 - u^2)/4$ and $N_{u\pm1} = 3(1 + u^2)/8$. At each emission, u and σ are simulated, and the application of the corresponding decay operator generates a translation of the momentum coordinate of the atom.

In the general three-dimensional case [4] the photon is identified with a direction vector $\boldsymbol{u}$ distributed on the unit sphere. There are two channels $\Lambda = \pm 1$ associated with the photon polarization, and this can be measured using any basis set $\boldsymbol{\epsilon}_{u\Lambda}$ orthogonal to $\boldsymbol{u}$. The decay operators are then given by

$$\hat{a}_{u\Lambda} = \sum_\sigma \boldsymbol{\epsilon}_\sigma \cdot \boldsymbol{\epsilon}^*_{u\Lambda}\hat{A}_\sigma \exp(-ik\boldsymbol{u} \cdot \hat{\boldsymbol{r}}), \tag{3}$$

where $\hat{\boldsymbol{r}}$ is the three-dimensional position operator. The standard polarization vectors $\boldsymbol{\epsilon}_\sigma$ correspond to the angular momentum of the emitted photon about the quantization axis of the atom.

In our new formulation the fluorescence is not measured directly but is instead observed through a lens. This is equivalent to the direct simulation of a Heisenberg microscope [6]. Applying a Fourier transform to the operators in Eq. (2) to model the action of the lens gives the new decay operators for one dimension

$$\hat{a}_{\nu\sigma} = \int_{-1}^{1} du\,(N_{u\sigma})^{1/2}\hat{A}_\sigma \exp[-iku(\hat{x} - \nu\lambda/2)], \tag{4}$$

where $\lambda = 2\pi/k$ is the photon wavelength. For angle resolved detection, u labels a continuous but bounded set of operators, so that in the conjugate basis, ν can be any integer and indexes an infinite set of operators at discrete points. The integral can be evaluated for $\hat{a}_{\nu=0\,\sigma}$ to give a localized function centered at the origin and the rest generated by translation by multiples of $\pm\lambda/2$. The emission time t' is chosen in the same way as for angle resolved detection [5]. The probability distribution from which ν and σ are simulated is then given by $\|\hat{a}_{\nu\sigma}\psi(t')\|^2$.

A physical constraint in considering three dimensions is that two parallel lenses must be used; one placed on each side of the object. We label these by $\zeta = \pm 1$, define the (x, y) plane to be the one aligned with the lenses, and use z to denote the perpendicular axis. The jump operators are found by transforming Eq. (3) to give

$$\hat{a}_{\nu\Lambda\zeta} = \sum_\sigma \int d\Omega_{\boldsymbol{u}}|u_z|^{-1/2}\boldsymbol{\epsilon}_\sigma \cdot \boldsymbol{\epsilon}^*_{u\Lambda}\hat{A}_\sigma \times \exp[-ik\boldsymbol{u} \cdot (\hat{\boldsymbol{r}} - \boldsymbol{\nu}\lambda/2)], \tag{5}$$

where the solid angle element $d\Omega_{\boldsymbol{u}}$ is in the direction $\boldsymbol{u} = (u_x, u_y, u_z)$ and the integration is over the hemisphere $u_z\zeta > 0$. In order to form a complete set of operators, the vector $\boldsymbol{\nu}$ is assigned the values $(\nu_x, \nu_y, 0)$ where ν_x and ν_y are integers. This indexes a two-dimensional lattice of possible cells with which the observed photon could be associated, each of size $\lambda/2$ by $\lambda/2$.

In Fig. 1 we illustrate the probability density resulting from the projection of a single photon measurement on a wave function in a momentum eigenstate. We have traced over the z direction and have used the circular polarization basis for $\boldsymbol{\epsilon}_{u\Lambda}$. The figure is the same for all choices of Λ and ζ. The probability falls off outside the characteristic unit wavelength scale in both pictures demonstrating the attenuation of the wave function at large distances from the observed photon position. This loss of spatial coherence by a single spontaneous emission has recently been observed experimentally by Pfau *et al.* [6]. Note that the wave function may spread coherently in between the localizing quantum jumps. In particular, in the case of near dark internal states which do not absorb and emit light frequently, the average spatial coherence length may be very large.

As a first example we apply the new operators to illustrate quantum position jumps in two dimensions. We consider a three level system in a Λ configuration. Spontaneous emission from the excited state $|e\rangle$ occurs predominantly to one of the ground states $|g_s\rangle$ on a strong transition with rate γ_s. This is much larger than the decay rate γ_w to the other ground state $|g_w\rangle$ on a weak transition. A resonant field with a large Rabi frequency Ω_s is used to saturate the strong transition. Population

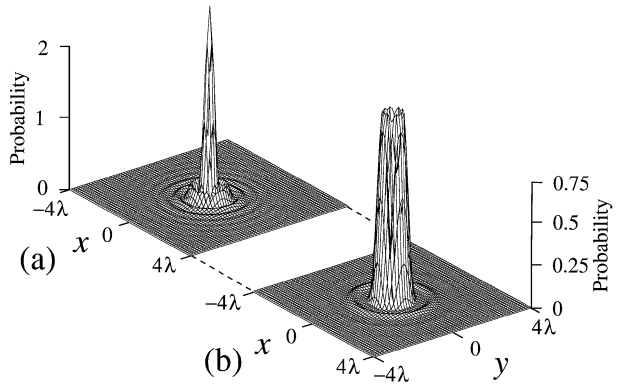

FIG. 1. The probability density of the state resulting from applying the localizing operators to a momentum eigenstate for $\nu = 0$ and for changes in magnetic quantum number during the transition (a) $\Delta m_j = 0$ and (b) $\Delta m_j = \pm 1$.

which accumulates in $|g_w\rangle$ is excited by a laser on the weak transition with a Rabi frequency Ω_w and a detuning $\Delta_w = \Omega_s$ equal to the Stark splitting of the excited state. A similar situation has been studied in the context of quantum jumps in ion traps where a single stored ion may exhibit periods of fluorescence on the strong transition interrupted by dark bands [7]. It has been shown that the dark periods are associated with the shelving of the electron on a weakly coupled state.

The periods of frequent photon emissions may localize the atomic center of mass wave packet according to the application of the new quantum jump operators. The dark periods in which no photons are detected are then associated with a free quantum diffusion of the wave function. In our model we consider two-dimensional motion on the (x, y) plane and the driving fields propagating along the z axis. In Fig. 2 we illustrate a sample trajectory in which we show the expectation value $(\langle\hat{x}\rangle, \langle\hat{y}\rangle)$ at times immediately after each of the spontaneous emissions. In this figure the time unit is ω_R^{-1} where the recoil energy is $E_R = \hbar\omega_R = \hbar^2k^2/2m$ and m is the atomic mass. The inset shows the sequence of quantum jumps indicated by vertical lines as a function of time. Analysis of the wave function shows that dark bands in the photon statistics produce a delocalized wave function so that the next localizing jump can be selected from a large region. This typically produces a long flight which can be seen in the periods denoted in the figure by a, b, and c. In order to observe these flights experimentally, it would be necessary to resolve the fluorescence from a single atom [8].

As a second application we consider the spatial diffusion of atoms in quantized optical molasses where laser cooling with counterpropagating light beams provides damping of the atomic motion and gives rise to spatial diffusion in a periodic optical lattice [9]. The temperatures achieved in experiments correspond to the accumulation of atoms in the few lowest vibrational energy levels of the optical potential which results in the localization of these atoms in space. A theoretical description of the random walk of an atom in the optical lattice should therefore be based on a fully quantum treatment of the atomic motion. We consider polarization gradient cooling in a 1D laser configuration consisting of two counterpropagating linearly polarized light waves with orthogonal polarizations driving an angular momentum $J_g = 1/2 \rightarrow J_e = 3/2$ and the more realistic $J_g = 3 \rightarrow J_e = 4$ transition [5]. In previous work [10] a spatial diffusion coefficient was calculated in a semiclassical approach which is restricted to a $1/2 \rightarrow 3/2$ transition and which neglects spatial localization in the potential wells.

Applying the localizing jump operators allows us to use a small spatial grid (covering typically 8 wavelengths, which, for the parameter values used in this Letter, turned out to be sufficient in order to account for the spreading to the wave function in between the localizing photon emissions) which dynamically traces the atom at each spontaneous emission. The propagation algorithm was the split-operator first Fourier transform [5]. One representative trajectory illustrating the random walk is shown in Fig. 3(a) where we plot the expectation value of the spatial coordinate as a function of time. The long periods when the position does not change appreciably correspond to sub-barrier motion when the total energy of the atom is below the threshold given by the maximum of the optical potential. Energy fluctuations allow the atom to eventually overcome the potential barrier which is indicated by the dashed line in Fig. 3(b). It may then travel over several wavelengths until it is trapped again. In Fig. 4(a) we plot the ensemble average over many trajectories illustrating the rate of expansion of the initially well localized cloud. Following the experimental

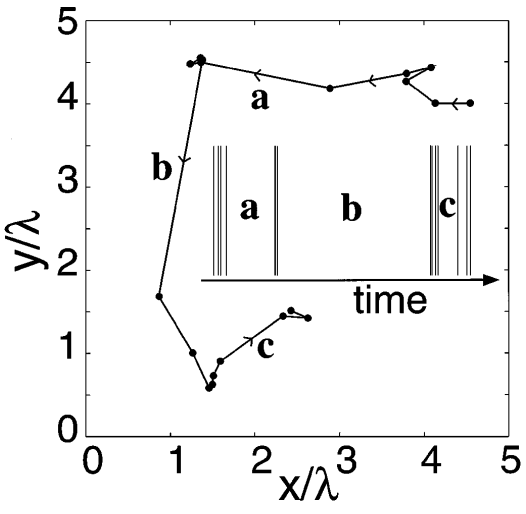

FIG. 2. Quantum jumps in position space. We show a sample trajectory for the expectation value of the wave packet for $\gamma_s = 8\,\omega_R$, $\gamma_w = \omega_R$, $\Omega_s = 1024\,\omega_R$, and $\Omega_w = 0.5\,\omega_R$. The inset shows the spontaneous emission times which appear on the trajectory as circles for a time interval $0 \le t \le 14\omega_R^{-1}$.

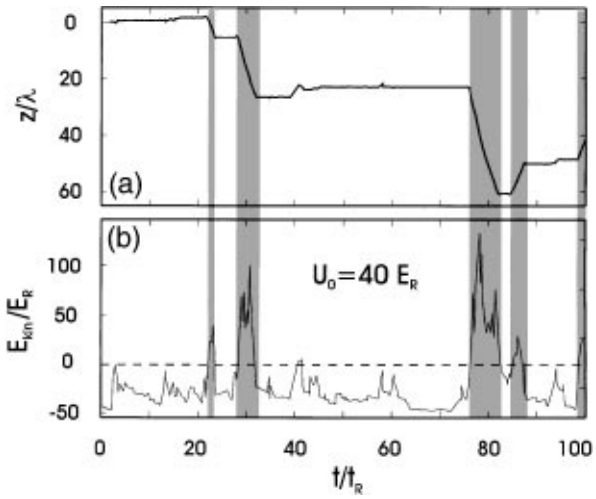

FIG. 3. (a) Expectation value of the spatial coordinate for a single trajectory vs time ($t_R = \omega_R^{-1}$) for $3 \rightarrow 4$. (b) Corresponding (kinetic plus potential) energy expectation value.

procedure in Ref. [10], we define a spatial diffusion coefficient as $(16\ln 2)^{-1}$ times the time derivative of the squared FWHM of the atomic distribution which for the final distribution in Fig. 4(a) is indicated by arrows. Note that in order to produce Fig. 4(a) with the angle resolved detection method we would need a 10 times larger (i.e., 80λ) spatial grid resulting in an approximately 14 times longer propagation time (we usually use a momentum grid ranging from $-32\hbar k$ to $+32\hbar k$). In the case of a $1/2 \rightarrow 3/2$ transition this factor increases to 60 for the same simulation parameters. Considering that a single run usually takes a couple of CPU days even when using several medium-size workstations, it is clear that the calculation of these diffusion coefficients is not feasible without the method of the localizing quantum jumps. This computational advantage becomes even more pronounced when we go to higher dimensions since the number of grid points scales as a power of the dimensionality of the problem.

The behavior of the spatial diffusion coefficient as a function of the potential depth U_0 [11] (the optical pumping rate γ_0 is kept constant) is plotted in Fig. 4(b) for a $1/2 \rightarrow 3/2$ transition (crosses) and a $3 \rightarrow 4$ transition (circles), and compared with the semiclassical theory for a $1/2 \rightarrow 3/2$ transition ignoring localization [10] (solid line). Both localization and going to higher angular momenta strongly suppress the spatial diffusion. This can be understood qualitatively by examining the distribution of kinetic energies in the molasses. From the upper two plots of Fig. 5 ($1/2 \rightarrow 3/2$) we find that 2.5% of all particles have kinetic energies that are large enough to overcome the potential barrier between neighboring potential minima [shaded area in Fig. 5(b)]. Those particles contribute the dominant part to the diffusion coefficient. A look at the lower two plots ($3 \rightarrow 4$) shows that only 0.5%, i.e., 5 times less than for the $1/2 \rightarrow 3/2$ transition, are now above the threshold given by the lowest adiabatic potential. Hence the strong suppression of spatial diffusion for this transition. A more detailed discussion of spatial diffusion in optical molasses, in particular, the existence of Lévy flights below a critical potential depth, will be published elsewhere [12].

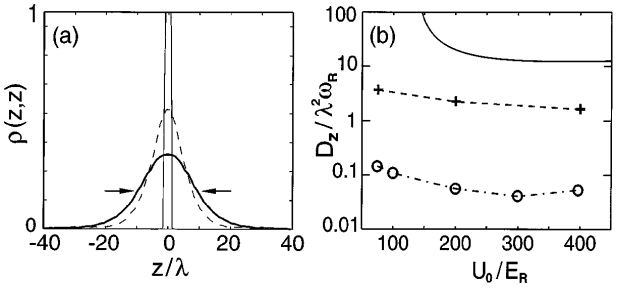

FIG. 4. (a) Spatial distribution at times $t = 0$, $500\omega_R^{-1}$, and $1000\omega_R^{-1}$ for $3 \rightarrow 4$, potential depth $U_0 = 200E_R$, and optical pumping rate $\gamma_0 = 3\omega_R$. (b) Spatial diffusion coefficient vs U_0 for $1/2 \rightarrow 3/2$ (+), $3 \rightarrow 4$ (o), and a semiclassical theory for $1/2 \rightarrow 3/2$ ignoring localization [10] (solid line).

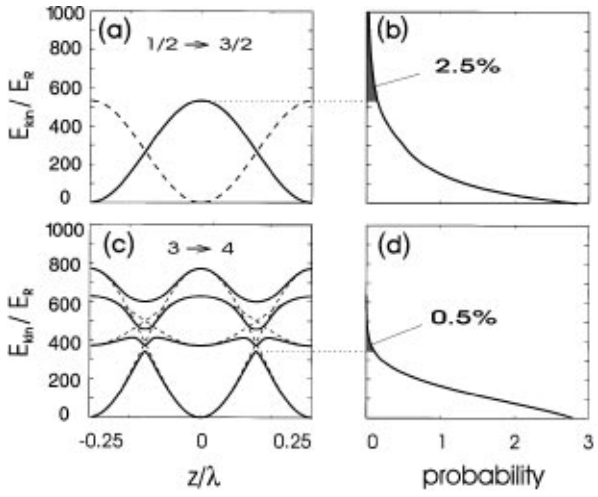

FIG. 5. (a) Optical potentials vs position for a $1/2 \rightarrow 3/2$ transition and $U_0 = 400E_R$. (b) Corresponding kinetic energy distribution. The dotted line divides below and above barrier energies. (c) and (d) same as (a) and (b) but for a $3 \rightarrow 4$ transition. The solid and dashed lines in (c) correspond to adiabatic and diabatic potentials, respectively.

This work was supported in part by the NSF and the Austrian Science Foundation.

[1] C. Gardiner, *Quantum Noise* (Springer, Berlin, 1991).
[2] A. Barchielli and V. P. Belavkin, J. Phys. A **24**, 1495 (1991).
[3] N. Gisin and I. C. Percival, Phys. Lett. A **167**, 315 (1992); B. M. Garraway and P. L. Knight, Phys. Rev. A **49**, 1266 (1994), and references cited.
[4] J. Dalibard *et al.*, Phys. Rev. Lett. **68**, 580 (1992); C. W. Gardiner *et al.*, Phys. Rev. A **46**, 4363 (1992); H. J. Carmichael, *An Open Systems Approach to Quantum Optics* (Springer, Berlin, 1993); N. Gisin and I. C. Percival, J. Phys. A **25**, 5677 (1992).
[5] P. Marte *et al.*, Phys. Rev. Lett. **71**, 1335 (1993); P. Marte *et al.*, Phys. Rev. A **47**, 1378 (1993); Y. Castin and K. Molmer, Phys. Rev. Lett. **74**, 3772 (1995).
[6] V. B. Braginski and F. Y. Khalili, *Quantum Measurement*, edited by K. S. Thorne (Cambridge University Press, Cambridge, 1992); S. M. Tan and D. F. Walls, Phys. Rev. A **47**, 4663 (1993); T. Pfau *et al.*, Phys. Rev. Lett. **73**, 1223 (1994).
[7] W. Nagourney *et al.*, Phys. Rev. Lett. **56**, 2797 (1986); J. C. Bergquist *et al.*, *ibid.* **56**, 1699 (1986); Th. Sauter *et al.*, *ibid.* **56**, 1696 (1986).
[8] Z. Hu and H. J. Kimble, Opt. Lett. **19**, 1888 (1994).
[9] See, for example, P. S. Jessen *et al.*, Phys. Rev. Lett. **69**, 49 (1992); G. Grynberg *et al.*, *ibid.* **70**, 2249 (1993); A. Hemmerich and T. W. Hänsch, *ibid.* **70**, 410 (1993).
[10] T. W. Hodapp *et al.*, Appl. Phys. B **60**, 135 (1995).
[11] We use the following definitions for the potential depth and the optical pumping rate: $U_0 = -\frac{1}{2s\Delta}$, $\gamma_0 = \frac{1}{4s\Gamma}$, where $s = \frac{2\Omega^2}{4\Delta^2+\Gamma^2}$.
[12] S. Marksteiner, K. Ellinger, and P. Zoller, Phys. Rev. A (to be published); see also F. Bardou *et al.*, Phys. Rev. Lett. **72**, 203 (1994).